

Synthesis and characterisation of new diindenodithienothiophene (DITT) based materials†

Irina Afonina,^a Peter J. Skabara,^{*a} Filipe Vilela,^a Alexander L. Kanibolotsky,^a John C. Forgie,^a Ashu K. Bansal,^b Graham A. Turnbull,^b Ifor D. W. Samuel,^b John G. Labram,^c Thomas D. Anthopoulos,^c Simon J. Coles^d and Michael B. Hursthouse^d

Received 21st September 2009, Accepted 17th November 2009

First published as an Advance Article on the web 15th December 2009

DOI: 10.1039/b919574b

Three new diindenodithienothiophene (DITT) based materials were synthesised and their electrochemical properties investigated. The HOMO–LUMO gaps were observed to be 3.33, 3.48 and 2.81 eV, respectively. Cyclic voltammetry results indicate increased stability for the alkylated derivatives. The dioxide exhibits strong photoluminescence, giving a photoluminescence quantum yield of 0.72 in solution and 0.14 in the solid state. Hole mobility measurements were carried out on the non-alkylated derivative and the corresponding values were $\sim 10^{-4}$ cm² V⁻¹ s⁻¹.

Introduction

Oligothiophenes, as a class of p-type organic semiconductor, attract considerable interest for their potential applications in OFETs, OLEDs and photovoltaics.^{1–3} This well-studied group of oligomers offers possibilities for fabricating electronic devices with higher stability, flexibility and lower cost of manufacturing. Fused oligothiophenes are often seen as analogs of oligoacenes such as pentacene, which is known for its high hole mobility.⁴ The study of new sulfur-containing fused structures is highly topical and concerns the development of synthetic methodologies,^{5–12} investigation of structure and electrochemical behaviour^{10,13} for utilisation in electronic devices such as organic transistors^{4,13–15} and light emitting diodes.^{16,17}

Fused thiophenes show larger HOMO–LUMO gaps in comparison with *e.g.* pentacene and this leads to their higher environmental stability^{6,16} and resistance to oxidation upon illumination. Also, fused thiophenes possess a rigid core structure with high planarity, which stimulates intermolecular assemblies in their solid state leading to highly ordered π – π stacking modes.^{5,6,9–13} On the other hand, linked oligothiophenes (and pentacene) adopt herringbone arrangements, which lower the degree of charge transport through the bulk material.^{4,9,11,18}

Generally, π – π stacking is favoured for a high C : H ratio within the π -framework of the molecule and, in the case of thiophenes, can be achieved through the fusion of rings; at the

same time, a higher density of sulfur enables more effective intermolecular interactions.^{7,11} Consequently, such ordered structures promote more efficient charge transport along the π -stacking direction and show good charge carrier mobilities, which play a crucial role for applications in *e.g.* OFETs.

The strong p-type character of fused thiophenes can be altered chemically through thienyl *S,S*-oxidation to produce materials with pronounced electron-acceptor features, such as lower LUMO energies (increased electron affinities) and increased electron delocalisation within the molecule.^{19,20} Also, strong photoluminescence, both in solution and in solid state, has been observed for a range of *S,S*-dioxy dithienothiophene derivatives,²¹ which can be useful for fabrication of emission based devices, such as OLEDs.

Dithienothiophene (DTT) is an important building block^{22–25} for the development of fused thiophene based semiconductors and offers possibilities for chemical diversity of materials for device applications. Herein, we present the synthesis of three new dithienothiophene based materials **4**, **5** and **6** and report their electrochemical and photophysical properties.

Results and discussion

Synthesis

Scheme 1 depicts the synthetic route to our new materials. The starting compounds **1**^{26–28} and **2**^{5,29} were prepared according to previously reported procedures. Our synthetic strategy is more efficient with compound **1**, but derivative **2** requires fewer steps to synthesise.

Diketone **3** was obtained as a mixture of diastereomers, which was confirmed by ¹H NMR. 2-Bromoindan-1-one (Aldrich) used in this reaction required additional purification by column chromatography (DCM–petroleum ether, 1 : 2, then DCM) since the high content of impurities in the commercially available chemicals resulted in the formation of by-products that were difficult to separate during subsequent purification procedures.

Cyclisation of the diketone **3** into a diindenodithienothiophene (DITT) **4** was successfully achieved using polyphosphoric acid. A

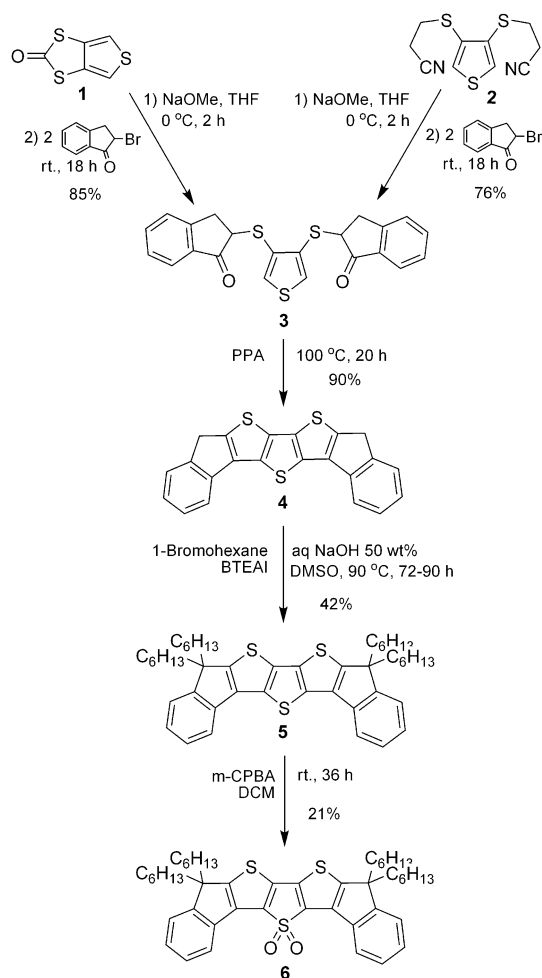
^aWestCHEM, Department of Pure and Applied Chemistry, University of Strathclyde, 295 Cathedral Street, Glasgow, UK G1 1XL. E-mail: peter.skabara@strath.ac.uk

^bOrganic Semiconductor Centre, SUPA, School of Physics & Astronomy, University of St Andrews, St Andrews, UK KY16 9SS

^cDepartment of Physics, Blackett Laboratory, Imperial College London, London, UK SW7 2BW

^dDepartment of Chemistry, University of Southampton, Highfield, Southampton, UK SO17 1BJ

† Electronic supplementary information (ESI) available: Experimental procedures and complete analyses for all new compounds, details of PLQY and fluorescence lifetime measurements. CCDC reference number 746672. For ESI and crystallographic data in CIF or other electronic format see DOI: 10.1039/b919574b



Scheme 1 Reactions and conditions for the syntheses of compounds 4–6.

few attempts to use P_2S_5 as the ring closing reagent were made but, due to its reductive effect, significant quantities of dihydrobisindenothiophene were isolated. Purification of **4** was performed either by recrystallisation from boiling toluene or by vacuum sublimation at 230 °C and 0.3 mmHg. The structure of **4** was confirmed by 1H NMR spectroscopy, mass spectrometry and elemental analysis. The X-ray crystal structure of **4** was also obtained.[‡] The solubility of unsubstituted DITT **4** was found to be quite poor in most common organic solvents (dichloromethane, diethyl ether, THF, CCl_4 , etc.). It dissolved very sparingly in hot (or boiling) chloroform, toluene, chlorobenzene and DMSO. Improvement of the solubility was therefore an important goal and alkylation of the aliphatic positions was chosen for this purpose.

Insertion of four hexyl chains was challenging, not only because of the poor solubility of **4**, but also due to the ineffectiveness of a number of bases used for its initial deprotonation. Applying bases such as butyllithium, NaOMe, LDA and

tetrabutylammonium hydroxide under various conditions promoted extensive degradation of **4** and produced extremely low yields of **5**. Finally, **5** was obtained using 50 wt% solution of NaOH and an interphase catalyst. Column chromatography (petroleum ether, 40–60 °C) was employed for purification.

Oxidation of **5** with *m*-CPBA produced a complex mixture of compounds and just over 20% of the highly photoluminescent product **6**. The pure material **6** was obtained by column chromatography (DCM–petroleum ether, 1 : 3) followed by precipitation with acetonitrile. Mass spectrometry results indicated the presence of two oxygens. 1H and ^{13}C NMR spectroscopy confirms the symmetry of the product, concluding that the two oxygens are positioned on the central thiophene unit. Such reactivity and regioselectivity have been shown previously in the oxidation of other DTT derivatives.²⁵ Compound **6** is quite soluble in most common organic solvents such as chloroform, DCM, THF, petroleum ether, toluene and chlorobenzene.

Electrochemistry

The electrochemical properties of materials **4**, **5** and **6** were investigated by cyclic voltammetry (CV) using dichloromethane as the solvent for oxidation and for the reduction of **6**. Tetrahydrofuran was required for the reduction of **4** and **5** at lower potentials. The supporting electrolyte was tetrabutylammonium hexafluorophosphate (0.1 M) and the potentials were referenced against the ferrocene/ferrocenium redox couple (Table 1 and Fig. 1). Glassy carbon was used as the working electrode with platinum and silver wires as the counter and pseudo-reference electrodes, respectively. Oxidation and reduction cycles were performed separately to avoid complications in the CV due to possible side products arising from irreversible and quasi-reversible processes. Compounds **4** and **5** gave very similar redox potentials with the main difference being that the oxidation of **5** was reversible (**4**, $E_{ox} = +0.72$ V and **5**, $E_{ox}^{1/2} = +0.68$ V). The hexyl chains blocking the α -position of the indene unit in **5** stabilise the radical cation intermediate, so we suspect that $4^{+•}$ undergoes chemical decomposition through reactivity at this position. The reduction of both compounds showed irreversible behaviour (**4**, $E_{red} = -2.86$ V and **5**, $E_{red} = -2.95$ V), indicating that the inclusion of hexyl groups did not stabilise the formation of radical anions. Analysis of **6** showed reversible peaks for both oxidation and reduction processes ($E_{ox}^{1/2} = +1.00$ V and $E_{red}^{1/2} = -1.99$ V); the increase in potential for the oxidation step was expected from the addition of the electron withdrawing sulfone group, but this adaptation of the structure gave the advantage of stabilising the reduction of the compound.

Generally, the incorporation of thienyl *S,S*-dioxide units into oligothiophenes leads to compounds that are more readily reduced than the corresponding oligothiophenes.³⁰

Absorption/emission studies

The UV-visible absorption spectra for all three compounds were measured in chloroform and are shown in Fig. 2 and S1 in the ESI† (see Table 1 for data). Compounds **4** and **5** show fine structure in the spectra, indicative of rigid, planar structures. Compound **6** shows a significant difference in comparison to the others; the main π – π^* transition is red shifted by ca. 140 nm due

[‡] Crystal data for **4** at 120(2) K with MoK α ($\lambda = 0.71073$ Å). Compound **2a**: $M = 372.50$, monoclinic, $P21/c$, $a = 15.8475(14)$, $b = 15.8514(14)$, $c = 6.9724(4)$ Å, $\beta = 98.498(6)^\circ$, $V = 1732.3(2)$ Å³, $Z = 4$, 19 708 measured reflections, 3940 unique reflections ($R_{int} = 0.1068$), $R = 0.1079$, $wR = 0.2819$.

Table 1 Electrochemical and electronic data for compounds **4–6** in solution

	$\lambda_{\text{abs, max}}/\text{nm}$	Optical $E_{\text{g}}^{\text{a}}/\text{eV}$	$\epsilon/\text{dm}^3 \text{ mol}^{-1} \text{ cm}^{-1}$	$\lambda_{\text{em, max}}/\text{nm}$	E_{ox}/V	E_{red}/V	HOMO ^c /eV	LUMO ^c /eV	Echem E_{g}/eV
4	284	3.4	34 300	373 (0.01) ^b	0.72 ^d	-2.86 ^d	-5.4	-2.1	3.3
5	273	3.4	56 600	376 (0.004) ^b	0.71/0.64	-2.95 ^d	-5.4	-1.9	3.5
6	419	2.6	32 100	524 (0.72) ^b	1.04/0.96	-2.03/1.95	-5.7	-2.9	2.8

^a Optical HOMO–LUMO gaps determined from the onset of the highest wavelength absorption band (and given in eV). ^b PLQY. ^c HOMO and LUMO values are calculated from the onset of the first peak of the corresponding redox wave and referenced to ferrocene, which has a HOMO of -4.8 eV. ^d Irreversible peak.

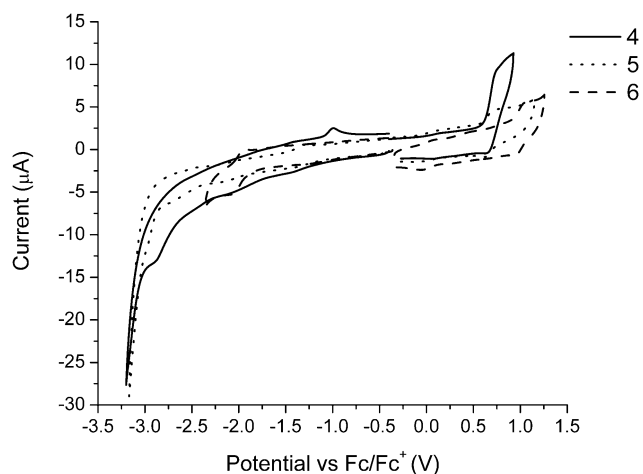


Fig. 1 Cyclic voltammograms of compounds **4–6**, using dichloromethane as the solvent for oxidation of **4–6** and for reduction of **6**, THF for reduction of **4** and **5**. The electrodes were glassy carbon, platinum wire and silver wire as the working, counter and reference electrodes, respectively. All solutions were degassed (Ar) and contained monomer substrates in concentrations *ca.* 10^{-4} M, together with *n*-Bu₄NPF₆ (0.1 M) as the supporting electrolyte. All measurements are referenced against the $E^{1/2}$ of the Fc/Fc⁺ redox couple.

to the electron withdrawing effect of the sulfone group, which narrows the HOMO–LUMO gap of the molecule. A spectroscopic study with a range of solvents was conducted that showed positive solvatochromism (see ESI†). Therefore, the large bathochromic shift seen for compound **6** may well originate from an intramolecular charge transfer process within the molecule.

The HOMO–LUMO gaps of **4**, **5** and **6** were determined from both the absorption spectra and the electrochemical data. The edge of the longest wavelength band corresponds to the optical HOMO–LUMO gap and this value was similar for **4** and **5**; compound **6** produced an optical HOMO–LUMO gap of 2.6 eV. The electrochemical HOMO–LUMO gaps were calculated from the differences in the onsets of the first oxidation and reduction peaks. Using data referenced to the ferrocene/ferrocenium redox couple, HOMO and LUMO energies were calculated by subtracting the onsets from the HOMO of ferrocene which has a known value of -4.8 eV. A summary of this data can be seen in Table 1. For all three compounds there is good agreement between optical and electrochemical estimates of the HOMO–LUMO gap. Compound **6** has a smaller electrochemical gap of 2.8 eV compared to **4** and **5** (3.3 and 3.5 eV, respectively).

Photoluminescence studies were performed on compounds **4–6** and the data are collated in Table 1 (see also Fig. 2 and S1 in the

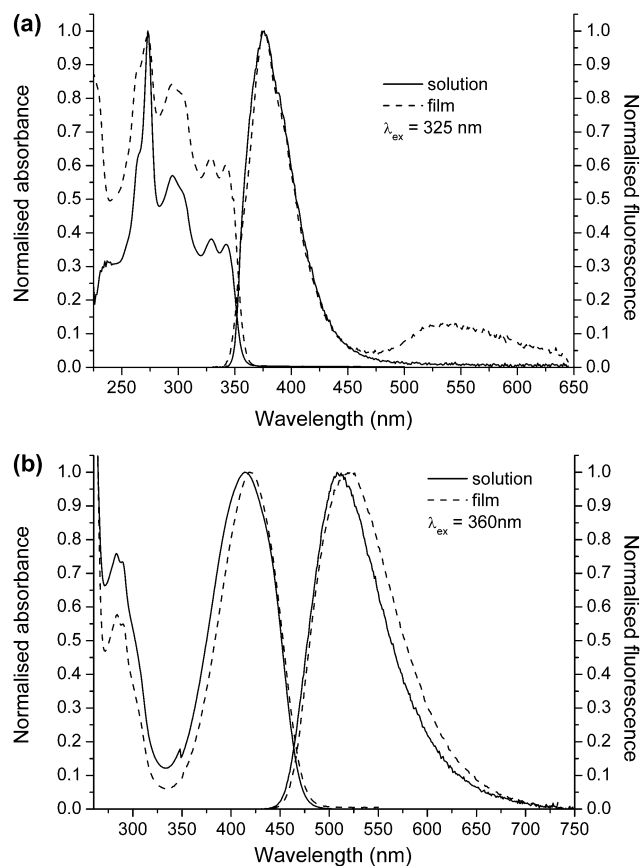


Fig. 2 Solution and solid state normalised absorption and emission spectra for compounds **5** (a) and **6** (b). Solution state spectra were recorded in chloroform.

ESI†). Solution studies of all three compounds were performed in dilute chloroform solution. Films of **5** and **6** were prepared on fused silica substrates by spin coating from chloroform solution. However, compound **4** was not sufficiently soluble to enable spin-coated films to be made. The four hexyl chains in **5** increase its solubility but reduce its PLQY (see ESI† and below). In films, the quantum yield could not be measured due to its weak emission. The film and solution spectra for **5** are similar, except the film shows an additional peak around 540 nm, indicating the presence of excimer emission (see ESI†). Compound **6** shows a strongly red shifted emission spectrum in comparison to **5**. It has a high PLQY in solution (72%). This is a far higher solution state photoluminescence quantum efficiency (PLQY) than related non-fused oligothiophene *S,S*-dioxide compounds,³¹ and we attribute this to the restriction of torsional flexibility.¹⁶

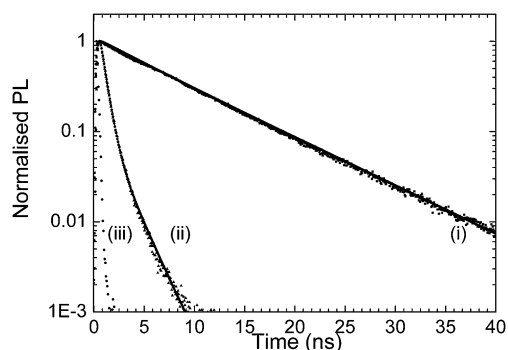


Fig. 3 Normalised PL decay of **6** with $\lambda_{\text{ex}} = 394$ nm (i) in solution at $\lambda_{\text{em}} = 524$ nm, (ii) in thin film made by spin coating inside the glove box from chloroform at $\lambda_{\text{em}} = 510$ nm and (iii) instrument response function.

Further information about the photophysics of compound **6** was obtained by making time-resolved photoluminescence (PL) measurements (Fig. 3). In solution, the PL decay was mono-exponential, with a lifetime of 7.9 ns. When combined with the PLQY of 0.72, this implies a natural radiative lifetime of 10.9 ± 1.1 ns. In the film the emission is quenched to 14%. The PL decay in the film is much faster, which we attribute to more rapid non-radiative decay, possibly due to the formation of aggregates. It can be fitted by two exponentials with lifetimes (preexponential factors) of 500 ps (79%) and 1.77 ns (21%).

X-Ray crystallography

Single crystals of compound **4** were isolated by recrystallisation from toluene. The asymmetric unit is shown in Fig. 4a and consists of seven fused rings labelled A–G. The central rings A–C represent the dithienothiophene unit and two benzene rings (F and G) are linked to this core *via* fused cyclopentadienes (D and E). The entire molecule is highly planar with the largest torsion angle in the structure being 2.19° within $S(2)–C(2)–C(3)–C(11)$. In the bulk, compound **4** forms one-dimensional π – π stacks (Fig. 4b) in which adjacent molecules are inverted but otherwise eclipsed (see Fig. 4c). Due to the curved shape of the molecules, this leads to rings A, D and E being efficiently overlapping with π – π ring centroid distances of 3.49–3.52 Å. Due to inversion between neighbouring molecules, rings B and C suffer from lateral displacement to give longer π – π distances (3.87 and 3.95 Å) and this is greatly exacerbated in the benzene rings F and G (5.03 and 4.75 Å), which reside at the peripheries of the curved structures.

Transistor fabrication and measurement

Despite the fact that we have designed the DITT-type compounds for photonic applications, the flat nature of the core structure led us to investigate the charge transport properties of compound **4**. We expected this compound to be the most favourable material in the series for charge transport properties due to the absence of the hexyl groups. Field-effect transistors were fabricated from compound **4** using heavily doped Si^{++} substrates as the gate electrode and a 200 nm thermally oxidised SiO_2 layer as the gate dielectric. Using conventional photolithography, gold source and drain electrodes were defined in

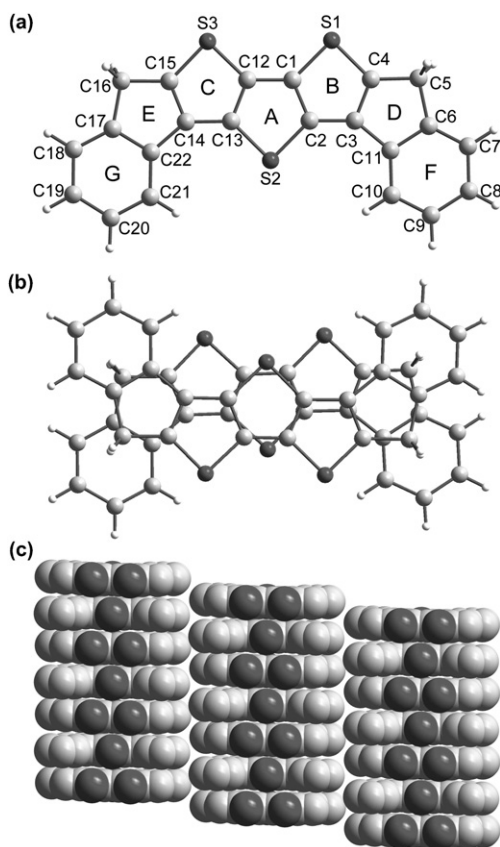


Fig. 4 (a) Asymmetric unit of compound **4** with labels; (b) inversion between a dimer of **4** within the one-dimensional stacks; and (c) space-filling diagram showing π – π stacking.

a bottom-contact configuration to give a channel length (L) of $15 \mu\text{m}$ and width (W) of $20 \mu\text{m}$. The SiO_2 layer was treated with the primer hexamethyldisilazane (HMDS) to passivate the surface. A 50 nm layer of the organic semiconductor was then deposited by vacuum sublimation at a base pressure of 10^{-9} bar and a rate of 1 \AA s^{-1} . Fig. 5a shows a polarised optical microscope image of material **4** vacuum deposited onto an HMDS treated Si/SiO_2 substrate, after annealing for 4 h at 125°C .

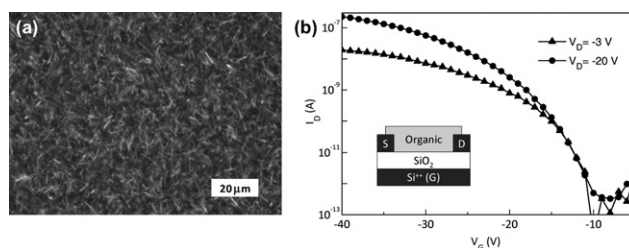


Fig. 5 (a) Polarised optical microscope image of material **4** vacuum deposited onto an HMDS treated Si/SiO_2 substrate, after annealing for 4 h at 125°C in nitrogen; and (b) transfer characteristics of bottom-gate, bottom-contact organic field-effect transistor ($L = 15 \mu\text{m}$ and $W = 20 \mu\text{m}$) based on compound **4** as the semiconductor layer. Transfer curves were measured at drain voltages of $V_{\text{D}} = -3$ V (triangles) and $V_{\text{D}} = -20$ V (circles). Inset shows schematic representation of the bottom-gate, bottom-contact transistor structure used.

Freshly prepared devices were then annealed at 125 °C for 4 h under atmospheric pressure in N₂. Electrical characterisation was carried out in N₂ at atmospheric pressure using a Keithley 4200 semiconductor parameter analyser.

Fig. 5b shows the transfer characteristics of a bottom-gate, bottom-contact field-effect transistor based on material **4**. The inset shows the schematic of the transistor structure employed. Transfer characteristics were obtained with the drain voltage (V_D) set to -3 V (linear regime) and -20 V (saturation regime). Using standard semiconductor models³² the hole mobility was calculated to be $\sim 10^{-4}$ cm² V⁻¹ s⁻¹. From plots of $I_D^{1/2}$ against V_G (not shown) the threshold voltage was determined to be approximately -21 V. The current on/off ratio and subthreshold slope for these devices were estimated to be $\sim 10^6$ and 2 V per decade, respectively. The relatively low hole mobility is attributed partly to the deep HOMO level of compound **4** and partly to the polycrystalline nature of the evaporated film (see Fig. 5a). It is anticipated that optimisation of the various evaporation conditions (*e.g.* evaporation rate, substrate temperature, *etc.*) could yield larger crystalline domains and hence higher charge carrier mobilities.

Summary

We have presented the synthesis of a new type of fused oligothiophene derivative and its functionalisation with solubilising and electron withdrawing side groups. Electrochemical, electronic absorption and photoluminescence studies indicate that the materials could be interesting components in extended structures for photonics applications. We are currently investigating the functionalisation of these materials further for incorporation into macromolecular conjugated structures.

Acknowledgements

We wish to thank the EPSRC for funding this work (EP/E027431, HYPIX: EP/F05999X, EP/F023200).

Notes and references

- 1 C. R. Mason, P. J. Skabara, D. Cupertino, J. Schofield, F. Meghdadi, B. Ebner and N. S. Sariciftci, *J. Mater. Chem.*, 2005, **15**, 1446.
- 2 Y. Shirota and H. Kageyama, *Chem. Rev.*, 2007, **107**, 953.
- 3 P. J. Skabara, R. Berridge, I. M. Serebryakov, A. L. Kanibolotsky, L. Kanibolotskaya, S. Gordeyev, I. F. Perepichka, N. S. Sariciftci and C. Winder, *J. Mater. Chem.*, 2007, **17**, 1055.
- 4 K. Xiao, Y. Q. Liu, T. Qi, W. Zhang, F. Wang, J. H. Gao, W. F. Qiu, Y. Q. Ma, G. L. Cui, S. Y. Chen, X. W. Zhan, G. Yu, J. G. Qin, W. P. Hu and D. B. Zhu, *J. Am. Chem. Soc.*, 2005, **127**, 13281.

- 5 E. Ertas and T. Ozturk, *Tetrahedron Lett.*, 2004, **45**, 3405.
- 6 M. He and F. Zhang, *J. Org. Chem.*, 2007, **72**, 442.
- 7 X. C. Li, H. Sirringhaus, F. Garnier, A. B. Holmes, S. C. Moratti, N. Feeder, W. Clegg, S. J. Teat and R. H. Friend, *J. Am. Chem. Soc.*, 1998, **120**, 2206.
- 8 J. J. Morrison, M. M. Murray, X. C. Li, A. B. Holmes, S. C. Moratti, R. H. Friend and H. Sirringhaus, *Synth. Met.*, 1998, **102**, 987.
- 9 T. Okamoto, K. Kudoh, A. Wakamiya and S. Yamaguchi, *Org. Lett.*, 2005, **7**, 5301.
- 10 R. M. Osuna, X. N. Zhang, A. J. Matzger, V. Hernandez and J. T. L. Navarrete, *J. Phys. Chem. A*, 2006, **110**, 5058.
- 11 L. San Miguel, W. W. Porter and A. J. Matzger, *Org. Lett.*, 2007, **9**, 1005.
- 12 X. N. Zhang, A. P. Cote and A. J. Matzger, *J. Am. Chem. Soc.*, 2005, **127**, 10502.
- 13 E. G. Kim, V. Coropceanu, N. E. Gruhn, R. S. Sanchez-Carrera, R. Snoberger, A. J. Matzger and J. L. Bredas, *J. Am. Chem. Soc.*, 2007, **129**, 13072.
- 14 Y. M. Sun, Y. W. Ma, Y. Q. Liu, Y. Y. Lin, Z. Y. Wang, Y. Wang, C. G. Di, K. Xiao, X. M. Chen, W. F. Qiu, B. Zhang, G. Yu, W. P. Hu and D. B. Zhu, *Adv. Funct. Mater.*, 2006, **16**, 426.
- 15 K. Yamada, T. Okamoto, K. Kudoh, A. Wakamiya, S. Yamaguchi and J. Takeya, *Appl. Phys. Lett.*, 2007, **90**, 072102.
- 16 G. Barbarella, L. Favaretto, G. Sotgiu, L. Antolini, G. Gigli, R. Cingolani and A. Bongini, *Chem. Mater.*, 2001, **13**, 4112.
- 17 I. F. Perepichka, D. F. Perepichka, H. Meng and F. Wudl, *Adv. Mater.*, 2005, **17**, 2281.
- 18 X. N. Zhang, J. P. Johnson, J. W. Kampf and A. J. Matzger, *Chem. Mater.*, 2006, **18**, 3470.
- 19 L. S. Miguel and A. J. Matzger, *J. Org. Chem.*, 2008, **73**, 7882.
- 20 Y. Suzuki, T. Okamoto, A. Wakamiya and S. Yamaguchi, *Org. Lett.*, 2008, **10**, 3393.
- 21 E. Tedesco, F. Della Sala, L. Favaretto, G. Barbarella, D. Albesa-Jove, D. Pisignano, G. Gigli, R. Cingolani and K. D. M. Harris, *J. Am. Chem. Soc.*, 2003, **125**, 12277.
- 22 J. Frey, A. D. Bond and A. B. Holmes, *Chem. Commun.*, 2002, 2424.
- 23 O. K. Kim, K. S. Lee, Z. Huang, W. B. Heuer and C. S. Paik-Sung, *Opt. Mater.*, 2003, **21**, 559.
- 24 G. Sotgiu, L. Favaretto, G. Barbarella, L. Antolini, G. Gigli, M. Mazzeo and A. Bongini, *Tetrahedron*, 2003, **59**, 5083.
- 25 G. Sotgiu, M. Zambianchi, G. Barbarella, F. Aruffo, F. Cipriani and A. Ventola, *J. Org. Chem.*, 2003, **68**, 1512.
- 26 L. Y. Chiang, P. Shu, D. Holt and D. Cowan, *J. Org. Chem.*, 1983, **48**, 4713.
- 27 M. A. Fox and H. L. Pan, *J. Org. Chem.*, 1994, **59**, 6519.
- 28 P. J. Skabara, K. Mullen, M. R. Bryce, J. A. K. Howard and A. S. Batsanov, *J. Mater. Chem.*, 1998, **8**, 1719.
- 29 P. Blanchard, B. Jousselle, P. Frere and J. Roncali, *J. Org. Chem.*, 2002, **67**, 3961.
- 30 G. Barbarella, L. Favaretto, M. Zambianchi, O. Pudova, C. Arbizzani, A. Bongini and M. Mastragostino, *Adv. Mater.*, 1998, **10**, 551.
- 31 L. Antolini, E. Tedesco, G. Barbarella, L. Favaretto, G. Sotgiu, M. Zambianchi, D. Casarini, G. Gigli and R. Cingolani, *J. Am. Chem. Soc.*, 2000, **122**, 9006.
- 32 J. Zaumseil and H. Sirringhaus, *Chem. Rev.*, 2007, **107**, 1296.